Interior Retrofit of Masonry Wall to Reduce Energy and Eliminate Moisture Damage: Comparison of Modeling and Field Performance

Peter Häupl, Dr.-Ing. **Heiko Fechner** **Hans Petzold**

ABSTRACT

In middle and northern Europe many existing buildings have to be improved energetically by means of additional thermal insulation on the building envelope. For buildings with façades worthy to be preserved, only an inside insulation layer may be possible, but with inside insulation layers, moisture problems often arise.

Using a capillary active material, as has been done in this research, the amount of condensation water on the cold side of the inside insulation can be reduced. Also, a vapor retarder is not necessary and, therefore, the drying potential is not limited.

Based on the physical models for coupled heat, air, water vapor, capillary water, pollutant, and salt transport (CHAMPS) in porous building and insulating materials and the computer code DELPHIN developed at the Institut für Bauklimatik (Dresden, Germany), in continuation of the topic "capillary active inside insulation," further substances and substance combinations were investigated in order to develop safe wall constructions in connection with appropriate thermal insulation. That was done via a computational prognosis and, secondly, with practical application in six test houses in Germany. The latter were connected to measurements of all climatic boundary conditions, such as temperature, relative humidity, shortwave radiation, precipitation, wind velocity and direction, as well as hygrothermic properties, such as temperature and humidity, in the materials.

For numerical simulation, a set of storage and transport functions for the porous building materials is necessary. This paper describes the modeling and measurement of the moisture storage and moisture transport functions for the capillary active insulation material "calciumsilicate" used in the study.

A comparison of measured and calculated hygrothermic performance within the envelope in a renovated frame house near Hannover, Germany, shows good correspondence. Heat losses have been reduced to one-third, and condensation water does not exceed 0.5 kg/m² during winter.

Moreover, a simplified computer code, COND, has been developed. It delivers about the same results and a sufficient assessment of the moisture distribution in the structure.

INTRODUCTION

After the necessary thermal renovation of a large number of houses and public buildings with external heat insulation systems in recent years, attention has moved on toward improvement of the thermal protection of monumental and protected buildings. The façades of such buildings usually must remain visible and unchanged due to their high historical value. A classic external insulation is therefore impossible. In order to be able to install a thermal improvement to decrease the energy consumption and to increase the living comfort, only internal insulation is possible.

Insulation on the inside increases the danger of condensation of penetrating water vapor within the construction. Each internal insulation layer should, therefore, be evaluated regarding this moisture risk. Correctly dimensioned vapor barriers can prevent the penetration of water vapor into the construction. However, they must be implemented very carefully in order to achieve also a durable tightness at critical points, such as impacts, corners, and penetrations. Experience

Peter Häupl is professor of building physics and managing director and **Heiko Fechner** and **Hans Petzold** are research associates at the Institute of Building Climatology, Faculty of Architecture, Dresden University of Technology.

shows that careless craft and, thus, risk potential remain. Particularly with framework constructions, another critical view of vapor barriers needs to be addressed: if dampness penetrates into the wall from the outside (driving rain by framework joints) or if built-in moisture is brought in by renovation measures, a vapor barrier would reduce the inward drying potential.

Additionally, today's interior climate can differ, sometimes strongly, from the climate present during construction. Nowadays, the required housing comfort usually causes higher interior air humidities and, thus, a stronger humidity load on the construction.

In terms of construction and moisture technology, one favorable alternative is interior thermal insulation without a vapor barrier but with a capillary-active insulating material. Possibly developing condensate is transmitted by the insulating material from the condensate layer to the room side and, thus, cannot damage the old construction. The liquid water mass in the construction can be limited to a harmless amount.

During recent years several renovations of buildings in Dresden (Gründerzeit building), Nuremberg (historical Herrenschiesshaus and community center Langwasser), and Senftenberg (permanent way and structures district building) were examined by the authors. Diffusion-open interior insulation systems with different materials were used.

In this context, the hygrothermic behavior of a capillary-active internal insulation in a half-timbered house in northern Germany is presented. With an installed instrument, the hygrothermic state variables are continuously measured at and within the construction. The building's climatic boundary conditions for the interior and outside air are used to validate the measurements by computations and to predict the rising condensation moisture volume and the drying behavior. Additionally, the effective heat transmission coefficient (U-factor) can be determined including all building climatic conditions, such as sun exposure, driving rain, heat storage, and phase conversion enthalpies. In the test house, a reduction by half of the heat transfer was reached without the necessity of a vapor barrier.

The calculation results presented here were obtained with the program DELPHIN for coupled moisture, air, and energy transfer in building materials and building parts. The program was developed at the Institute for Building Climatology at the Dresden University of Technology. The thermodynamic basics and the function of the program are described in Grunewald (1998). For a description of the moisture-technical material parameters, a coherent analytic model is available (Grunewald et al. 2003; Häupl and Fechner 2003). On the basis of the pore radius distribution, expressions for the moisture storage and moisture transport function arise as a result of integration. These are nonlinear functions, which can be described mathematically for the entire moisture range (dry to saturated). The material parameters were determined for the most part in laboratory measurements at the Institute for Building Climatology and in cooperating European research institutions.

The research results—practical experiences, material parameter determination, simulation—also allow the evaluation of newly erected constructions and other reorganization variants regarding their long-term thermal and hygric behavior.

TEST BUILDING DESCRIPTION

Half-timbered houses are common in many areas of Germany. Buildings with a visible framework front are often protected as monuments due to their aesthetics and historical importance. However, the usage requirements of today often differ strongly from those of the construction period. The external framework walls provide limited thermal protection, which affects comfort and heating costs negatively, and due to their small thickness can lead in critical cases to surface condensation with fungal growth. The internal insulation of the construction with a capillary-active insulating material represents a meaningful solution. Possible condensate can be capillary transported to the warm side of the construction, whereby the moisture load of the construction is reduced. The drying process of winter condensate and possible built-in moisture is substantially supported (Fechner et al. 1999; Häupl et al. 2003).

The half-timbered house in Edemissen Eickenrode near Hannover, Germany, discussed in this article, is representative of a number of framework constructions with framework infill of clinker. The infill has only small thermic protection so that additional insulation is absolutely necessary to avoid surface condensation (the U-factor of the original infill is only 2.2 W/m^2 K and does not fulfill the requirements for minimum thermic protection). During reorganization of the first floor walls, calcium silicate insulation was projected internally. Although the authors had experience with the reorganization of a half-timbered building in East Saxony (Häupl 2003), the monument protection authority wished an instrumented monitoring of the construction components regarding moisture risks. Therefore, three measuring points in the first floor were selected. In order to also simulate the measurements during a period of several years, an additional measuring device was installed. Thus, climatic parameters of the interior and outside air, as well as state variables, were measured at surfaces and within the external walls.

With the measured data, it was possible to judge the moisture performance of the overall construction as well as the examined construction components. Since the influence of building use on the wood moisture and/or the possible condensation moisture volume is quantifiable by measurement of the interior climate, basic conditions for future use can be indicated. Further statements could be made regarding the energy consumption (U-factor improvement by internal insulation).

The half-timbered house examined (Figure 1) is a large rural residential building. The ground floor consists of brickwork, the upper floor and gable walls of the attic are of frame construction (oak framework with brick infill), and the west front (weather side) is additionally covered with wood boards.

Figure 1 *View of the test house from the street side (northeast).*

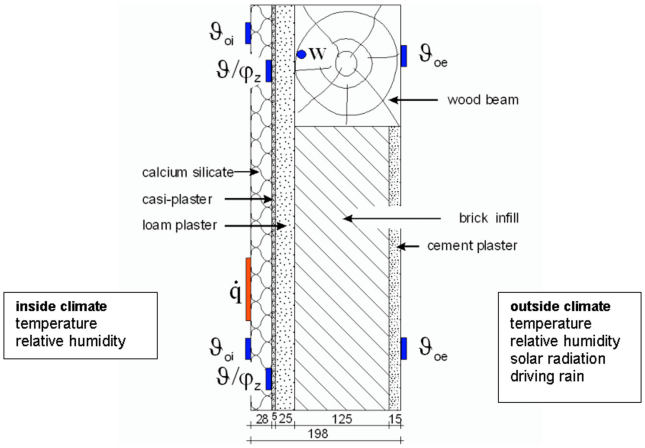

Figure 2 *Wall construction with sensors in the infill and at the wooden beam.*

The house possesses a corridor in the ground floor and in the first upper floor in the longitudinal direction (axis east-west); on the eastern side are the stairs. The attic is designed as a ventilated roof. In the ground floor, the kitchen, living rooms and a small bath, as well as office space are situated. In the first upper floor are sleeping and living rooms and on the eastern side a larger bath with a sauna.

On the north side is a guest room, also with bath, which is only rarely in use.

BUILDING CLIMATIC MEASUREMENTS

For direct measurement of wood moisture content, electrical resistance measurement was employed. The necessary electrodes were brought in through the insulation into the respective wood construction components. Further, the relative humidities and temperatures of the outside and room air were measured on the cold side of the insulating layer with capacitive probes, the surface temperatures outside and inside with Ntc and/or Pt100-sensors, and the heat flow density with a heat flow plate 12×12 cm. The measurement of rain, wind, and radiation could be abstained from in this test house. For the simulation, measured values of the outside surface temperature sensors include the radiation effect and temperature influences due to solar radiation and precipitation. Missing climatic data can be completed by values of the test reference year for Bremerhaven. The load by driving rain is small due to the large roof projection.

The bath on the eastern side is used regularly by the inhabitants. It also contains a sauna, so that substantial moistening and heat points occasionally occur. This is regarded as the most critical hygrothermic area so the most extensive measuring equipment was installed here. The results of the measurements and the associated simulation results will be described later.

In order to be able to reconstruct the two-dimensional framework wall, within the range of the infill (brickwork) and the range of a framework bar, measurements were performed separately. Figure 2 shows the wall construction with the sensors in the infill and at the beam.

The results of the measurements for the outside temperature and outside air humidity are not presented here. In the summer temperatures were only briefly higher than 30°C. In the winter of 2000/2001 the minimum temperature was approximately –5°C; in the winter of 2001/2002 the temperature fell briefly below –10°C. Altogether the measured winter climate can be classified as relatively mild.

The measured outside relative humidity shows the usual yearly process with a shorter period of higher air humidities during the winter; the average value of the humidity lay in the cold period at around 90%.

MODELING

The modeling of the coupled heat and moisture transfer can be expressed by the following nonlinear differential equation system for the calculation of temperature and moisture fields in building materials and building structures (Häupl and Stopp 1987; Grunewald 1998; Künzel 1994; Funk and Grunewald 2002; Bomberg et al. 2002).

$$\frac{\partial}{\partial t}\begin{bmatrix}(\rho_M c_M + \rho_w c_w w)\cdot T + (\rho_v c_{pV} + \rho_A c_{pA})\cdot (w_s - w)T \\ \rho_v h_v (w_s - w) - u_{source}\end{bmatrix}$$

$$= \frac{\partial}{\partial x_k}\begin{bmatrix}\left(\lambda + \delta e^{-\frac{p_c}{\rho_w R_v T}}(h_v + c_{pV}T)\cdot\left[\frac{\partial p_s}{\partial T} + \frac{p_s p_c}{\rho_w R_v T^2}\right]\right)\frac{\partial T}{\partial x_k} \\ + \left(Kc_w T + \delta e^{-\frac{p_c}{\rho_w R_V T}}(h_V + c_{pV}T)\cdot\frac{p_s}{\rho_w R_v T}\right)\frac{\partial p_c}{\partial x_k}\end{bmatrix} \quad (1)$$

$$\frac{\partial}{\partial t}[(\rho_w w + \rho_v(w_s - w)) - \rho_{w.source}]$$

$$= \frac{\partial}{\partial x_k}\left[\begin{array}{l}\left(K + \delta e^{-\frac{p_c}{\rho_w R_V T}}\frac{p_s}{\rho_w R_v T}\right)\frac{\partial p_C}{\partial x_k} \\ + \delta e^{-\frac{p_c}{\rho_w R_V T}}\left(\frac{\partial p_s}{\partial T} + \frac{p_s p_c}{\rho_w R_v T^2}\right)\frac{\partial T}{\partial x_k}\end{array}\right] \quad (2)$$

The left-hand side of Equations 1 and 2 contains the time derivation of the storage functions for heat and moisture; the right-hand sides are the divergences of the heat and moisture flow densities. As driving potentials the temperature T and the capillary pressure p_c—which means actual thermodynamic potentials—have been used. The capillary pressure p_c and the vapor pressure p_v correspond with the waterfilled pore radius by the well-known equations, Equations 3 and 4.

$$p_c = \frac{2\sigma}{r} \quad (3)$$

$$p_v = p_s(T)e^{-\frac{2\sigma}{r \cdot \rho_w \cdot R_V \cdot T}} \quad (4)$$

In order to solve the transport equation system (Equations 1 and 2) by given initial and boundary conditions (usually the hourly values of the climate components temperature, relative humidity, short- and longwave radiation, wind speed, wind direction, and precipitation—driving rain), the material functions $c(w(p_c), T)$ and $w(p_c), T$ for the storage and $\lambda(w(p_c), T)$, $K(w(p_c), T)$ and $\mu(w(p_c), T)$ for the transport are necessary. This paper uses the definition and determination of the moisture storage function $w(p_c)$ and the liquid moisture conductivity $K(w(p_c))$ and the vapor transport function $\delta(w(p_c))$ in the isothermal case, though a lot of practical nonisothermal cases with the DELPHIN code have been solved (Häupl 1999; Häupl et al. 2001; Fechner 2001).

The fundamental idea is to represent the pore size distribution by means of a function with suitable parameters. The moisture storage function is given by a simple integration of the pore size distribution. The parameters can be identified by the measurement of the capillary pressure function with the pressure plate apparatus in the overhygroscopic range and the sorption isotherm in the hygroscopic range. The moisture transport functions can be formulated by means of the equilibrium of capillary pressure and friction pressure. In addition to the measurement of the storage function, the measurement of the moisture conductivity for saturated samples, the water uptake and water penetration coefficient, and the water vapor coefficient for $\phi = 20\%$ and $\phi = 85\%$ is sufficient to determine the parameters of the transport function.

Moisture Storage Function

As criterion for the representation of the pore structure, the pore size distribution $f(r) = dw/dr$ or $f_p(r) = dw/d(\log r)$ will be used. It can be measured by mercury porosimetry, BET-method, etc. For an analytical description of the pore size distribution, the following formulations were deemed good after many tests.

$$f_{pn}(r) = \sum_{j=1}^{m} \frac{4.6 \cdot \left(\frac{r}{R_j}\right)^2 w_{nj}(n_j - 1)}{\left[1 + \left(\frac{r}{R_j}\right)^2\right]^{nj}} \quad (5)$$

Equation 5 contains the partial volume w_{nj} and the main radius R_j of the pore size compartment as parameters and in addition the shape parameter n_j describing the width of the distribution function. In general $m = 3$ or $m = 4$ packages are sufficient (three or four modal models). Up to now about 30 building and insulation materials have been assessed. The moisture loading process up to the filled radius r can be described by the integration of Equation 5.

$$w(r) = \int_0^r \frac{fp(r)}{r} 0.4343\, dr \quad (6)$$

The integration of Equation 5 gives Equations 7 and 8.

$$w_n(r) = \sum_{j=1}^{m} \left(1 - \left(1 + \left(\frac{r}{R_j}\right)^2\right)^{1-nj}\right) w_{nj} \quad (7)$$

The moisture content (Equation 7) resembles the formulation of van Genuchten (1999).

Hence, it follows with the capillary pressure (Equation 3),

$$w_n(p_c) = \sum_{j=1}^{m} \left(1 - \left(1 + \left(\frac{2\sigma}{p_c R_j}\right)^2\right)^{1-nj}\right) w_{nj} \quad (8)$$

In the last equation the dependence of the moisture content w on the capillary pressure p_c can be seen. In the overhygroscopic range ($p_c < 5 \cdot 10^6$ Pa) Equation 8 is identical with the capillary pressure function; in the hygroscopic range ($p_c > 5 \cdot 10^6$ Pa) Equation 8 is identical with the sorption isotherm. The sorption isotherm follows by means of Equation 4.

$$p_c = \rho_w R_v T \cdot \ln(\varphi) \quad (4)$$

$$w_n(\varphi) = \sum_{j=1}^{m} \left[w_{nj} \cdot \left(1 - \left(1 + \left(\frac{2\sigma}{\rho_w R_v T \cdot \ln(\varphi) R_j}\right)^2\right)^{1-n_j}\right)\right] \quad (9)$$

The moisture storage function can be measured and the simple parameters R_j and w_j can be identified (see example calciumsilicate and measurement results in Equation 8).

Moisture Transport Functions

In the isothermal case, Equation 2 yields the liquid moisture flow density.

$$g_w = -K_w(\rho_c) grad\ p_c \qquad K_w \text{ in s} \tag{10}$$

$K_w(p_c)$ is the liquid moisture transport function or moisture conductivity. The driving potential is the capillary pressure p_c. Under the assumption of a bundle of parallel capillaries with gaps for the pressure compensation, the equilibrium between the capillary pressure and the friction pressure results in (compare Equation 9)

$$g_w = \left[-\frac{\rho_w \cdot M}{8\eta} \left[\int_o^r f_p(r) r\ dr \right] \right] grad\ p_c\ . \tag{11}$$

Hence, it follows for $K_w(p_c)$,

$$K_w(p_c) = +\frac{\rho_w \cdot M}{8\eta} \int_o^r f_p(r) r\ dr\ . \tag{12}$$

In order to simulate a mesh of non-regular pores with different moisture transport resistances (Roels 2000), a number of background calculations with different friction forces were done.

The following method has been obtained: The unknown details of the pore structure will be included by the measurement of moisture conductivity K_s for saturated samples by means of a small outside pressure difference p_o (Darcy-permeability), which means

$$K_w(p_o) = -\frac{\rho_w M}{8\eta} \int_o^{r_o} f_p(r) r\ dr = K_s \qquad p_o = \frac{2\sigma}{r_o}\ . \tag{13}$$

The integration of Equation (12) is possible with the chosen formulation of the pore size distribution (Equation 5). This is the most important advantage compared to Van Genuchten. From (Equation 13) with (Equation 5) it follows for the moisture conductivity (Equation 15),

$$r = \frac{2\sigma}{p_c} \qquad r_o = \frac{2\sigma}{p_o} \tag{14}$$

$$K_{wn}(p_c) = K_s \cdot \frac{\sum_{j=1}^{m} \left[1 - \frac{1 + n_j \left(\frac{r}{R_j}\right)^2 + (n_j - 1) \cdot \left(\frac{r}{R_j}\right)^4}{\left[1 + \left(\frac{r}{R_j}\right)^2 \right]^{n_j}} \right] \cdot \frac{R_j^2 w_{nj}}{n_j - 2}}{\sum_{j=1}^{m} \left[1 - \frac{1 + n_j \left(\frac{r_o}{R_j}\right)^2 + (n_j - 1) \cdot \left(\frac{r_o}{R_j}\right)^4}{\left[1 + \left(\frac{r_o}{R_j}\right)^2 \right] n_j} \right] \cdot \frac{R_j^2 w_{nj}}{n_j - 2}} \tag{15}$$

With the simple parameters R_j (main radius of the pore segment), w_{nj} (partial volume of the pore segment), and K_s (Darcy-permeability) the liquid moisture conductivity in the whole range (from absolutely dry to completely saturated) can be formulated. Of course with Equation 8 or 9 the moisture conductivity in dependence on the moisture content w can be represented, but, unfortunately, only implicitly. Moreover the parallel P and serial (1-P) configuration of the moistened pores gives an additional resistance. The capillary conductivity (Equation 15) has to be multiplied with

$$\kappa(P, w_n(r)) = \frac{P}{P + (1 - P) \cdot \left(1 - \frac{w_n(r)}{w_s}\right)^2} \tag{16}$$

$$K(p_c, P) = \kappa(P, w_n(r)) \cdot K_{wn}(p_c)\ . \tag{17}$$

In the next step, the moisture conductivity K should be transformed into the moisture diffusivity D_w. It is defined by

$$g_w = -\rho_w D_w(w) grad w\ . \tag{18}$$

The comparison of (Equation 18) with (Equation 10) gives for D_w,

$$D_w(r) = 4.6 \cdot \frac{K_w(r)}{f_p(r)} \cdot \frac{\sigma}{r \rho_w}\ . \tag{19}$$

Moreover, the so-called water uptake coefficient is well known and fixed in the ISO standard 15 148.

$$\frac{m_w}{A} = A_w \sqrt{t} \tag{20}$$

A sample will be brought in direct contact with a water surface. The increase of the mass m_w per cross section area A caused by the water penetration will be measured. Hence, it follows A_w. It is also possible to measure the penetration depth x_E of the water front and, consequently, the water penetration coefficient.

$$x_E = B \sqrt{t} \tag{21}$$

This simple integral experiment is suitable for a partial control of the storage and transport functions in the numerical simulation of the penetration fields with the DELPHIN code (Grunewald 1998).

In this paper also a simplified analytical formulation for the moisture diffusivity D_w based on the parameters of Equations 20 and 21 will be proposed. For the isothermal case and missing moisture sources, the moisture transfer equation (1) reads as follows:

$$\frac{\partial}{\partial t} w(x,t) = \frac{\partial}{\partial x} \left[D_w(w) \frac{\partial w}{\partial x} \right] \tag{22}$$

The driving potential p_c is substituted by the water content w. The formulation (Equation 23) has approximately the same

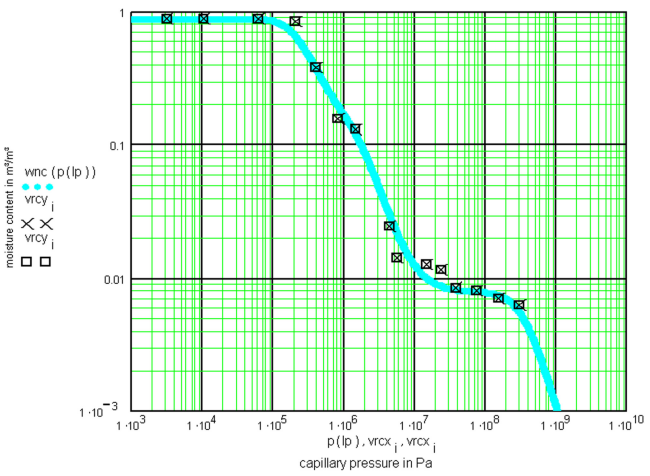

Figure 3 *Comparison of calculated and measured water retention function of the material.*

shape as the function (Equation 17) (compare example calciumsilicate).

$$D_{wu}(w) = D_o\left[\left(1-\frac{w-w(\varphi_o)}{w_{sf}-w(\varphi_o)}\right)^{\frac{1}{k}-1} - \left(1-\frac{w-w(\varphi_o)}{w_{sf}-w(\varphi_o)}\right)^{\frac{2}{k}}\right] \tag{23}$$

The analytical solution of Equation 22 with Equation 23 for the simple water uptake experiment is given by Equation 24.

$$w(x,t) = (w_{sf}-w(\varphi_o))\left[1-\left(\frac{1}{\sqrt{2D_o(k+1)}}\frac{x}{\sqrt{t}}\right)^k\right] + w(\varphi_o) \tag{24}$$

The moisture field can also be measured (see calciumsilicate in Figure 11) and the solution (Equation 24) can be confirmed. The parameter D_o moisture diffusivity for

$$w \approx \frac{w_{sf}+w(\varphi_0)}{2} + w(\varphi_0) \tag{25}$$

and k (shape parameter) in Equation 23 can be calculated by means of the water uptake coefficient A_w and moisture penetration coefficient B and by the fitting of the measured moisture penetration field, respectively.

For $w = w(\varphi_o)$ Equation 24 results in the penetration depth x_E, and the time integration about the field (Equation 24) delivers the increase of the whole moisture content m_w/A. Hence, it follows for k and D_o,

$$k = \frac{A_w}{\rho_w(w_{sf}-w(\varphi_o))B - A_w} \tag{25}$$

Table 1. Coefficients of the Water Retention

j	w_{nj} (m^3/m^3)	R_j (m)	n_j (-)
1	0.0120	$1.14\cdot10^{-04}$	3
2	0.2247	$6.00\cdot10^{-06}$	3
3	0.0010	$1.30\cdot10^{-07}$	3
4	0.0073	$5.60\cdot10^{-10}$	3

$$D_o = \left[\frac{A_w}{\rho_w(w_{sf}-w(\varphi_o))}\right]\frac{k+1}{2k^2}. \tag{26}$$

The example calciumsilicate confirms this procedure. Of course, the moisture diffusivity (Equation 23) can be transformed by means of (Equation 19) in the moisture conductivity and can be compared with (Equation 16).

Example: Insulation Material Calciumsilicate

Basic Physical Parameters and Material Properties.

Surface tension of water	$\sigma = 0.074$ N/m
Density of water	$\rho_w = 1000$ kg/m³
Water vapor constant	= 462 Ws/kg K
Temperature	$T = 293$ K
Conductivity for saturated material	$K_s = 1.763\ 10^{-8}$ s
Parallel placement of pores	$P = 0.5$
Water uptake coefficient	$Aw = 0.146$ kg/m² s $^{1/2}$

Vapor diffusion resistance coefficient for dry material $\mu_o = 3.5$

Pore Size. Figure 3 shows the measured values for the water retention function. The parameters of the water retention function (see Table 1) have been calculated by making use of a nonlinear approximation algorithm. In this case, the exponent n of the storage function is always 3. The pore size distribution function has been calculated by deriving the moisture retention function (Equation 7).

Liquid Moisture Transport Functions—Moisture Conductivity *K* and Moisture Diffusivity *D*

The moisture conductivity (Equation 15) has been calculated by integrating the moisture retention function (Equation 8). Therefore, the conductivity contains the same parameters as in Table 1. Additionally, the moisture conductivity for the saturated material *Ks* and the structural parameter *P* has been used. Figure 4 shows the conductivity in dependence on the water content.

The moisture diffusivity is given by Equation 19 and in approach by Equation 23. In the classical way, the water uptake coefficient *Aw* and the water penetration coefficient **B** have been measured.

A_w = 1.19 kg/m²s$^{1/2}$
w_{sf} = 0.83 m³/m³
B = 0.00193 m/s$^{1/2}$

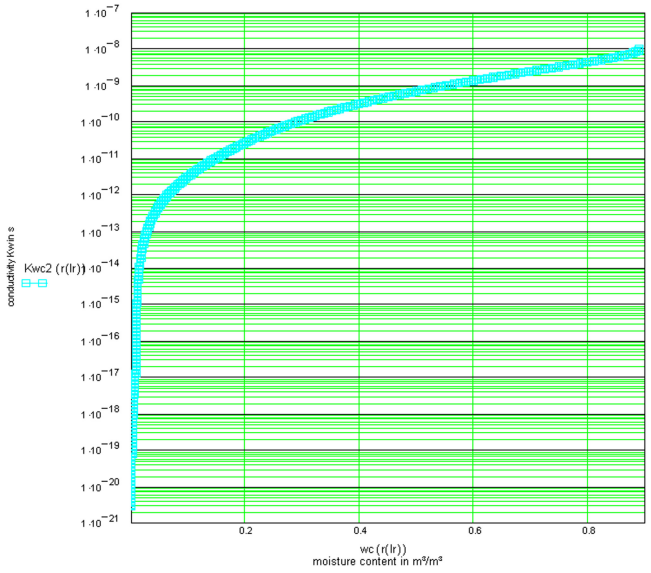

Figure 4 *Liquid moisture transport function K(w) in dependence on water content.*

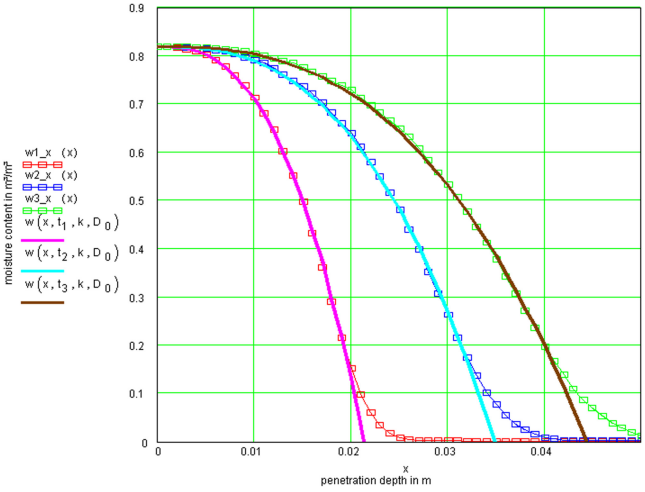

Figure 5 *Measured and fitted moisture penetration field for calciumsilicate.*

From that, the values *Do* and *k* follow:

$Do = 4.68\ 10^{-7}$

$k = 2.99$

Moreover, the moisture field is measured by X-rays (Roels et al. 2004)—see Figure 5—and the parameters $Do = 3.453\ 10^{-7}$ and $k = 2.661$ are given by the regression procedure with Equation 24 of these field curves.

Figure 6 contains the diffusivities calculated by means of the pore size distribution (Equation 19) (grey curve Dwc2) and the approximating curves Equation (23) by *Aw* measurement *Dwcu* and by field measurement *DwcL*. The correspondence of these diffusivities is quite good.

The model is also suitable to describe the moisture capacity and moisture conductivity of wood. The moisture retention function (Equation 8) delivers, together with the Darcy value *Ks*, the basic conductivity (Equation 15). The parallel part in Equation 16 is in fiber direction approximately 0.6, normal to the fiber direction only 0.01. The anisotropic properties follow from this.

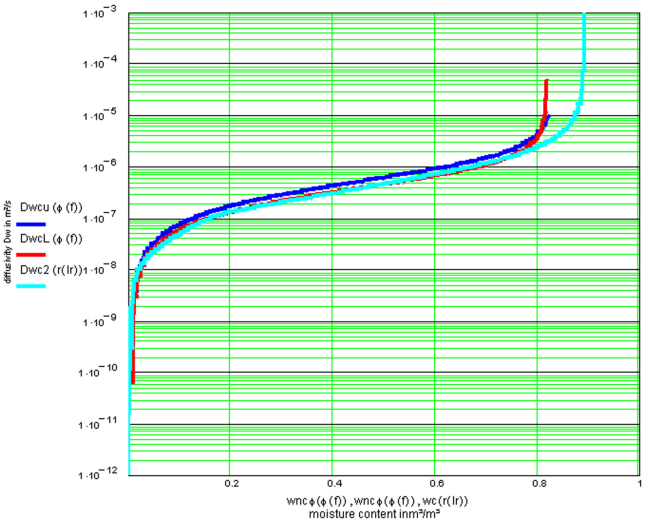

Figure 6 *Liquid moisture transport function-moisture diffusivity by pore size distribution and by water uptake experiments.*

RESULTS OF MEASUREMENT AND NUMERIC SIMULATION

The thermic values—course of the heat flux and the measured temperatures in the level insulation/old construction in the infill—can be well reconstructed as expected by one- and two-dimensional calculations. The maximum heat flow density through the wall is approximately 30 W/m^2 K. High summer temperatures of the external surface caused by radiation in the warm season also lead to heat flows into the inside. The temperature behind the insulation remains in the cold season over the frost limit (Figure 7).

From the average values of the temperature difference and heat flow in the cold season, a U-factor of 1.25 W/m² K can be determined for the construction (measurements include the solar radiation and the instationary procedures). That corresponds to approximately half of the original value of 2.2 W/m² K before the thermal retrofitting.

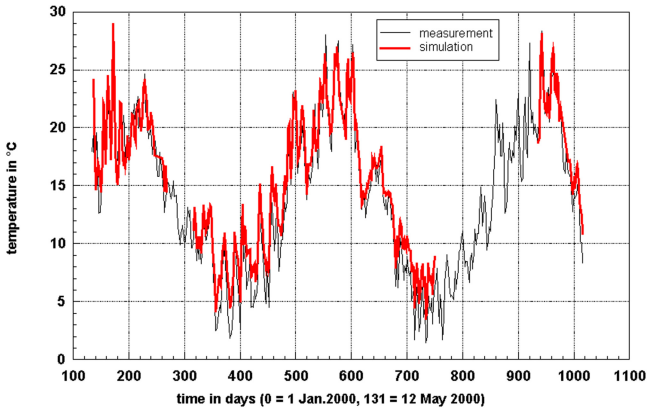

Figure 7 *Measured and calculated temperature at the cold side of the insulation layer in the infill, bathroom east, 12 May 2000-14 October 2002.*

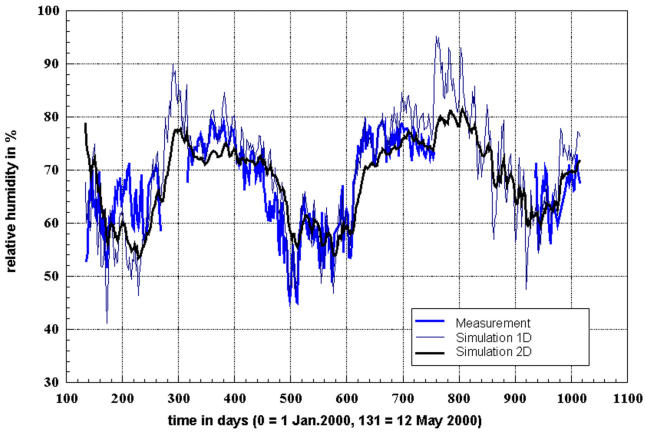

Figure 8 *Measured and calculated relative humidity on the cold side of the insulation layer in the infill, bathroom east, 12 May 2000-14 October 2002.*

The humidity between internal insulation and old construction is represented in Figure 8. The two-dimensional calculation shows thereby the measured values better than the one-dimensional calculation. Particularly in the second condensation period, a very good agreement between two-dimensional calculation and measurement is to be noted. The correspondence speaks for the quality of the simulation code DELPHIN.

The critical humidity of 80% (above which during longer time periods mold growth can occur at appropriate temperatures [Viitanen 1997]) is not exceeded in the measurement and only briefly in the calculation. Also, in the winter only slightly higher values occur in 2001/2002.

The computation shows that there are still reserves in the moisture-technical regard. An increase of the insulation thickness is, however, not recommended, since the room air dampness could easily be higher in the bathroom with more intensive use and less ventilation. In the context of future renovation measures, the exchange of the original windows is planned against tighter ones, which entails a higher interior humidity. The rule of thumb "halving of the original U-factor" for the capillary-active internal insulation is thus also valid here.

The maximum wood moisture in the condensation period during the monitored time occurred at the border wood infill. The wood moisture never rises over 9 Vol% or 16.4 M% and is thereby clearly under the critical parameter of 18 M% for the fiber saturation.

Since no hygric problems arise in the construction under the load of measured climate, additionally an increase of the interior air humidities was modeled and examined while maintaining the measured external climate.

In those calculations with the program DELPHIN4 a constant interior temperature of 20°C and two constant room air humidities with 60% and 70% were assumed. The assumption of a room air humidity of 70% can be regarded thereby as an extreme load.

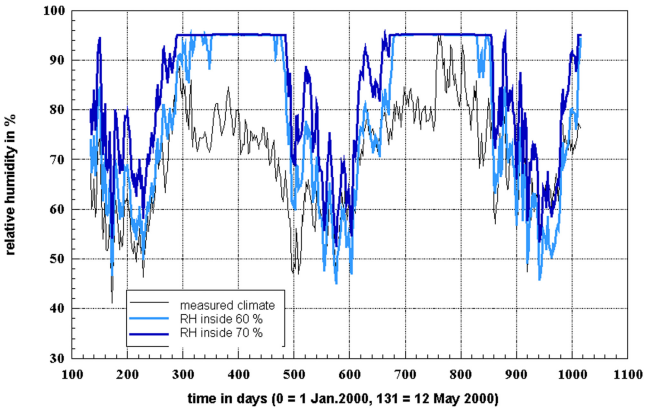

Figure 9 *Relative humidity between calcium silicate insulation and old wall in the infill bathroom east, natural climate and two constant interior climates with* θ_i *= 20°C (one-dimensional calculations), 12 May 2000-14 October 2002.*

Figure 9 shows the air humidities on the cold side of the insulation for measurement and the two assumed inside climates. While in the natural case there is a maximal rise of 88%, for 60% interior humidity 95% is reached so that the formation of liquid water begins.

The water mass with the interior model relative humidities, resulting from condensation, reached $\varphi_i = 70\%$ briefly, a maximum of 0.3 kg/m²; with $\varphi_i = 60\%$ the maximal amount is 0.15 kg/m² (Figure 10). Nevertheless, the drying takes place quite fast. The field of the moisture profile over the time in Figure 11 (1D field) shows for the case of 60% inside relative

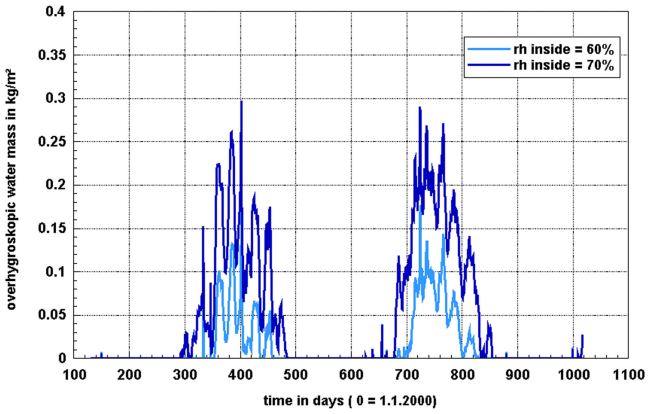

Figure 10 *Overhygroscopic moisture content in the infill bathroom east, natural climate and two constant interior climates with* θ_i = 20°C *(one-dimensional calculations), 12 May 2000-14 October 2002.*

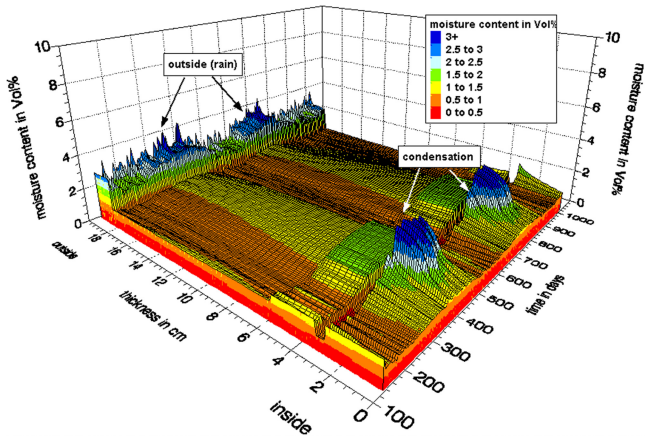

Figure 11 *One-dimensional moisture field in the infill bathroom east; constant interior climate* θ_i = 20°C, φ_i = 60 %, *12 May 2000-14 October 2002.*

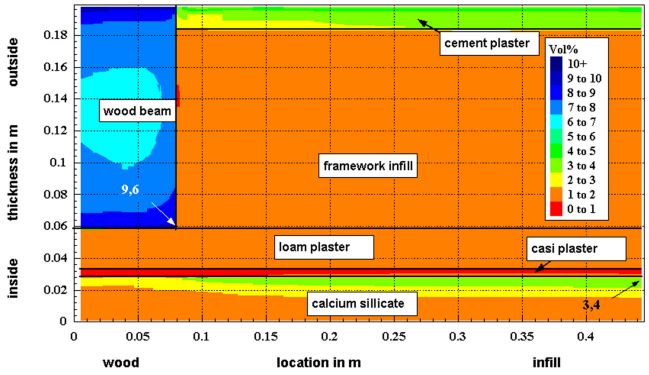

Figure 12 *Two-dimensional moisture field in the east bathroom at 6 February 2001 (day 402); constant inside climate* θ_i = 20°C, φ_i = 60%.

humidity, the condensation as well as the transport process of the condensate to the room side and the quick drying process after the end of the winter period (material moisture content in the capillary active calcium silicate insulation over 2 Vol%, represented as blue in the figure). Without capillary conductivity the moisture content would be increased to approximately 2.9 kg/m².

The situation at the timber beam must be regarded again as a two-dimensional problem. The most critical place is the internal corner of the wooden beam; because of the smaller thermic protection of the framework infill, the temperatures are lowest there. Figure 11 shows the two-dimensional -moisture field on 28 April 2001 (day 483), the day on which the highest humidity content in the beam corner occurred. The beam experiences a relatively high moisture content at the border to the infill due to the higher heat transfer there. The maximum values of the wood moisture amount to between 9 and 10 Vol%. With a wood gross density of 550 kg/m³, the wood moisture remains thus in each case under 18 M%, the beginning of the critical range for the formation of mold.

CALCULATION FOR THE EXTERNAL WALL ACCORDING TO EN ISO 13788/DIN 4108

In addition to the framework infill in the east bathroom, calculations according to DIN 4108 shall be presented. The simple program COND and the climatic values presently favored in the DIN committee (Θ_i = 20°C/ φ_i = 50% as well as Θ_e = – 5°C/ φ_e = 80%) are used.

Since the calculated procedure according to Glaser, which is used in DIN 4108 and the European standard EN ISO 13788, does not consider the capillary characteristics of the building materials, this computation obtains 4.9 kg/m² condensate. However, this does not correspond under any circumstances to reality. Calcium silicate plates are used as internal insulation because of their strong liquid water conductivity, which means they can transport condensate and ease the situation substantially, as shown earlier.

The simple planning software COND (Häupl et al. 2001) considers the moisture conductivity and storage in contrast to the standards above. Figure 12 shows the input format—the user must input the structure and assign the materials from a list. For the selected constant climatic boundary conditions, a temperature and moisture profile is returned as both tabular and graphical output.

The condensation moisture mass, with consideration of all moisture-technical characteristics, thus amounts to 0.43 kg/m² and thus lies in the permissible range. For the wall with internal insulation, results show a U–factor of 1.17 W/m² K.

TU Dresden
Institut für Bauklimatik
Programm: Cond 2002 - v1.3.4 Registriert für: Häupl

05.01.2004

FRAME WORK - INSIDE INSULATION

Cross section

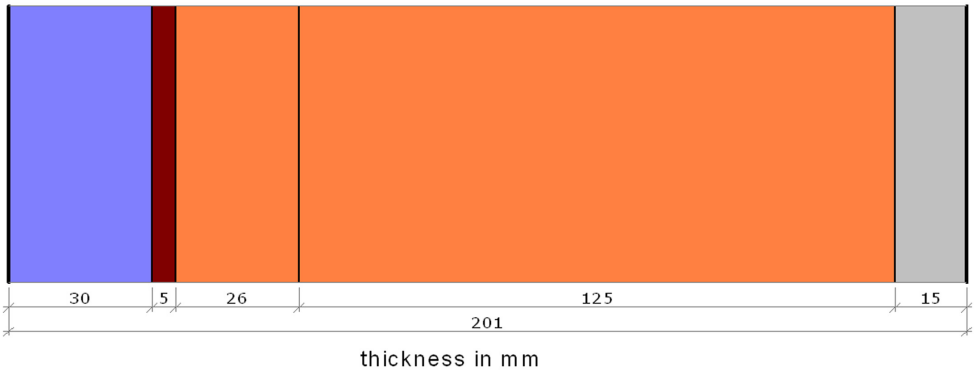

thickness in mm

Structure and material parameters

	Material	d [mm]	λ [W/mK]	μ [---]	w_{hyg} [m³/m³]	w_{sat} [m³/m³]	A_w [kg/m²s^{0,5}]
1	calciiumsilicate	30	0,0650	4,0	0,008	0,850	0,7760
2	layer of adhesive	5	1,3000	32,0	0,010	0,330	0,0400
3	loam plaster	26	0,8700	12,0	0,020	0,350	0,2000
4	clinker	125	0,9500	25,0	0,007	0,270	0,0300
5	lime cement plaster	15	0,9800	21,0	0,025	0,300	0,0250

Climate data

Winter

Indoor climate		Outdoor climate	
Temperatur	18,5 °C	Temperatur	0,5 °C
Relative Luftfeuchte	60,0 %	Relative Luftfeuchte	85,0 %

Condensation period 90 days

Summer

Indoor climate		Outdoor climate	
Temperatur	18,0 °C	Temperatur	15,0 °C
Relative Luftfeuchte	60,0 %	Relative Luftfeuchte	70,0 %

Drying period 90 days

Surface resistances

Internal surface R_{si} = 0,130 W/m²K
External surface R_{se} = 0,040 W/m²K

Figure 13 *Input table and results of the calculation with the software COND.*

Temperature, vapour pressure, moisture content

	Schicht/Material	θ [°C]	P_{sat} [Pa]	P [Pa]	w [m³/m³]	d_c [mm]	M_c [kg/m²]
	Luftschicht (links)	18,5	2130	1278			
		15,5	1763	1278			
1	calciiumsilicate				0,006		
					0,034	12,7	0,22
		5,6	908	908			
2	layer of adhesive				0,020	5,0	0,04
					0,017		
		5,5	903	903			
3	loam plaster				0,027	26,0	0,19
					0,028		
		4,8	861	861			
4	clinker				0,013	5,8	0,02
					0,006		
		1,8	695	569			
5	lime cement plaster				0,020		
					0,020		
		1,4	677	539			
	Luftschicht (rechts)	0,5	634	539			

Summary of results

Heat transition coefficient (moist structure)	U =	1,279	W/(m²K)
Heat transition coefficient (dry structure)	U =	1,231	W/(m²K)
Condensation water at the end of the condensation period	M_c =	0,476	kg/m²
Hygroscopic loading time	t_{hyg} =	0,77	d
Overhygroscopic loading time	t_c =	29,90	d
Drying time	t_{ev} =	6,15	d

Temperature and moisture profil

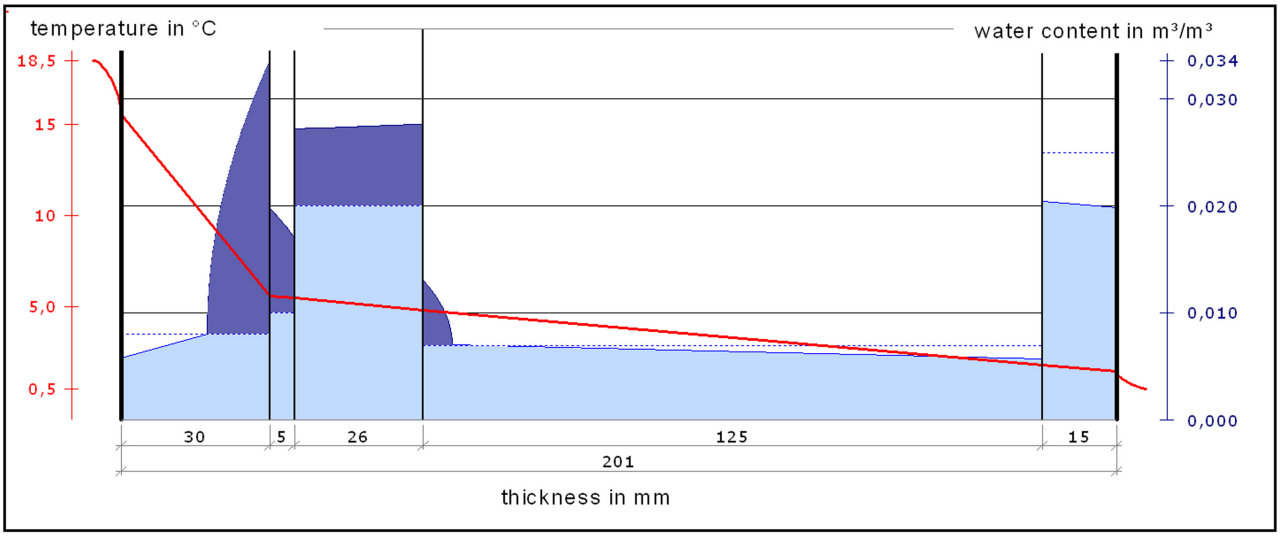

Figure 13 (continued) *Input table and results of the calculation with the software COND.*

SUMMARY AND OUTLOOK

Based on two years of measured data, the validation, and additional simulation computations, the function of the investigated construction can be evaluated positively. The moisture content of the framework wood on the room side is, at all three measuring sections, in the uncritical range below fiber saturation. This is supported by measurements of the humidity within the construction. Obviously the capillary-active calcium silicate internal insulation serves its purpose. Its potential is not fully used due to the relatively mild external climate and the moderate interior climate. The remaining reserves are, however, meaningful with regard to future renovation measures.

The U-factor of the refurbished wall is indicated by COND as 1.17 W/m^2 K and is thus halved in relation to the condition before the renovation. This shows very good agreement with the effective U-factor determined for heat flow and surface temperature of 1.13 W/m^2 K. The effective value includes the solar radiation. Furthermore, the thermal storage effect over the entire heating season (1 October to 30 April) is negligible.

The condensate volume determined with COND after 90 days under constant climate conditions is 0.450 kg/m^2 under the critical limit of 1 kg/m^2 for insensitive constructions and also under 0.5 kg/m^2 for sensitive constructions. In the case of a calculation done according to EN 13788 of DIN 4108 (Glaser scheme), without consideration of the capillarity and hygroscopicity, a condensate volume of 4.9 kg/m^2 results, which would be inadmissible. However, both the measurements and the computations with the instationary software program DELPHIN-4 show that the construction does not show hygric problems and, consequently, the proof after Glaser is to be classified as unrealistic. The construction is further a good example for the fact that with capillary active building materials such as calcium silicate the capillary water conductivity may not be neglected.

The example calculations with increased interior air humidities show that the wall construction remains functional even with a stronger moisture load. Even during the strongly increased interior climatic load of 70% relative humidity, according to the COND calculation (constant outside climate and 20°C air inside temperature) no more than 0.731 kg/m^2 condensate occurs in the infill, and according to the DELPHIN calculation (measured external climate), only 0.289 kg/m^2. In the most critical place for the timber beam—the cold side of the insulation and corner to the framework infill—a maximum of 9.6 Vol% (which corresponds with a wood density of 550 kg/m^3 17.5 M%) is still an acceptable wood moisture content.

The energetic effects of the internal insulation are satisfying. The U-factor of the construction could be halved without the necessity of installing a vapor barrier. Thus, a good drying potential, which is important for framed walls, remains. A further decrease of the U-factor to 0.8 W/m^2 K by using a thicker insulating layer would be possible.

Comparison of the measurements with the results of the numeric simulation shows good agreement. The results also can be transferred in a general manner to other constructions, although the specific conditions must be considered individually in every case (see also Häupl et al. 2002). The kind of the wall construction, the local inside and outside climate, and, particularly for historical buildings, the materials used all should be considered carefully.

REFERENCES

Bomberg, Pazera, Haghighat, Grunewald, 2002. Modified cup for testing of water vapour transmission through thick permeable materials. 6th Symposium on Building Physics in the Nordic Countries, Trondheim, Norway.

Fechner, Grunewald, Häupl, Martin, Neue, Petzold, 1999. Hygrothermisches Verhalten von Fachwerkbauten mit zusätzlicher Innendämmung. Wissenschaftliche Zeitschrift der TU Dresden 2/1999.

Grunewald, J. 1998. Diffusiver und konvektiver Stoff- und Energietransport in kapillarporösen Baustoffen. Dissertation TU Dresden.

Funk, Grunewald, 2002. Physical assumptions and derivation of transport coefficients in the thermodynamical model of the Heat and Moisture Transport Simulation Program DELPHIN4. Journal of Building Physics, Slovak Academy of Sciences, Bratislava.

Grunewald, Häupl, Bomberg, 2003: Towards an Engineering Model of Material Characteristics for Input to HAM Transoprt Simulations. Journal of Thermal Envelope and Building Science 4/2003, SAGE Publications.

Häupl, Stopp, 1987. Feuchtetransport in Baustoffen und Bauwerksteilen. Dissertation B, TU Dresden.

Häupl, Fechner, Stopp,2001. Ein einfaches Verfahren zur feuchtetechnischen Bemessung von Außenbauteilen. Dresdner Bauklimatische Hefte. Heft 7, TU Dresden.

Häupl, Stopp, Petzold, 2002: Thermische Sanierung von Fachwerkwänden mittels kapillaraktiver Innendämmung. In: Fachwerkinstandsetzung nach WTA, Band 2. Fraunhofer IRB Verlag.

Häupl, Fechner 2003. Hygric material properties of porous building materials. Proceedings of the 2nd international conference on building physics. Balkema Publishers.

Häupl, Jurk, Petzold 2003. Inside thermal insulation for historical facades. Proceedings of the 2nd international conference on building physics. Balkema Publishers.

Künzel, 1994. Verfahren zur ein- und zweidimensionalen Berechnung des gekoppelten Wärme- und Feuchtetransports in Bauteilen mit einfachen Kennwerten. Dissertation Uni Stuttgart.

Roels. 2000. Modelling unsaturated moisture transport in heterogeneous limestone. KU Leuven.

Roels et al. 2004. A comparison of different techniques to quantify moisture content profiles in porous building materials. *Journal of Thermal Envelope and Building Science*, 4/2004, Sage Publications.

van Genuchten 1999 (Editor). Proceedings of the International Workshop on Characterization and Measurements of the Hydraulic Properties of Unsaturated Porous Media 1997. Riverside, California, 1999.

Viitanen, H. 1997. Modelling the time factor in the development of mould funghi - the effect of critical humidity and temperature conditions on pine and spruce sapwood. In: Holzforschung Vol. 51. Walter de Gryuter Verlag..